Potts model on a fractal lattice

1987 J. Phys. A: Math. Gen. 20 2159

(http://iopscience.iop.org/0305-4470/20/8/029)

J. Phys. A: Math. Gen. **20** (1987) 2159-2178. Printed in the UK

Potts model on a fractal lattice

Pik-Yin Lai and Yadin Y Goldschmidt

Department of Physics and Astronomy, University of Pittsburgh, Pittsburgh, PA 15260, USA

Received 9 July 1986

Abstract. We consider the dilute Potts model on the Sierpinski carpet. The model has a phase transition at a finite temperature and both critical and tricritical behaviour are observed for $q < q_c$ (where q is the number of Potts states). We use Migdal-Kadanoff type recursion relations to obtain the value of q_c and of critical and tricritical exponents and investigate their dependence on various geometrical characteristics of the fractal.

1. Introduction

In recent years there has been much interest in the properties of fractal objects (Mandelbrot 1982) which appear in various areas of physics like aggregation, percolation, turbulance and many more (Mandelbrot 1982). One direction of study has been to consider the critical properties of spin systems of fractal lattices (Gefen *et al* 1983a, b, 1984). It has been found that the Ising model on a fractal displays a phase transition of finite temperature only when the order of ramification (Mandelbrot 1982) of the fractal is infinite. Besides its fractal dimension, the fractal lattice is characterised by other geometrical properties like connectivity and lacunarity (Mandelbrot 1982) and the question is how these characteristics affect the critical behaviour of spin models on fractals (Gefen *et al* 1983c, 1984). A complete answer to this question has not been given.

In this paper we consider the Potts model on the Sierpinski carpet (Mandelbrot 1982). On a hypercubic lattice the Potts model is characterised by a value q_c, where q is the number of Potts states, below which the transition is second order and above which it is first order. It is of interest to find out how q_c, and how critical exponents for $q < q_c$, depend on the properties of the fractal. The Potts model on the carpet has been considered in the past (Riera and Chaves 1986), but the authors used the Migdal-Kadanoff renormalisation group for the pure model, to be distinguished from the dilute Potts model. It is well known (Nienhius *et al* 1979), the even on the hypercubic lattice one has to incorporate vacancies into the Potts model in any real space renormalisation group (RG) treatment otherwise q_c cannot be detected (the transition is always second order) because the symmetry between the coexisting phases is not respected by the RG transformation. Also the values of the exponents for $q < q_c$ but close to q_c are not accurate without incorporating dilution. Thus in this paper we consider the dilute Potts model on the fractal lattice. This enables us also to obtain the exponents at the tricritical point which exists for the dilute model, including the Ising tricritical point which has not been investigated previously. We use the Migdal-Kadanoff (Migdal 1975, Kadanoff 1976) RG method to investigate the critical properties of the model, since an analytic method is not available at this point. The method has

0305-4470/87/082159+20$02.50

the drawback that, because it is only approximate, it is not always clear which of the results originate from inaccuracies of the method and which are intrinsic to the model.

2. Properties of Sierpinski carpets

We summarise here briefly the properties of the fractal lattices which are being considered in this work, namely the Sierpinski carpets (Mandelbrot 1982, Gefen *et al* 1984) embedded in two Euclidean dimensions. They are constructed in the following way: we start with a square of unit area which we divide into b^2 equal subsquares out of which l^2 are eliminated. For given (b, l), there are many ways to eliminate the l^2 squares. We consider the cases where 90° rotation symmetry is preserved. The construction is repeated iteratively for each square in a self-similar way until one reaches the 'microscopic' length scale.

The fractal dimension of the carpet is given by

$$D = \ln(b^2 - l^2)/\ln b. \tag{2.1}$$

Hence $1 < D < 2$. The topological dimension of the carpet (Mandelbrot 1982) is given by $D_T = D'_T + 1$, where D'_T is the topological dimension of the 'cutset'. Since the carpet can be cut by a Cantor set, whose topological dimension is zero, it follows that the topological dimension of the carpet is 1, which is less than the fractal dimension D, as is expected for a fractal.

The order of ramification R of a fractal lattice at a point P is the supremum of the number of significant bonds which one must cut in order to isolate an arbitrarily large bounded set of points connected to P (Mandelbrot 1982, Gefen *et al* 1984). For the carpets which are considered here $R = \infty$. When spin models which display a finite-temperature phase transition on a regular translationally invariant lattice are put on the fractal lattice with $R = \infty$ they display a finite temperature transition as well (Gefen *et al* 1984), as opposed to the same model on a fractal with finite order of ramification which displays a transition only at zero temperature (Gefen *et al* 1983a, b).

The connectivity Q is defined as $Q = \min\{D'\}$, where D' is the fractal dimension of the surfaces of isolated bounded sets (Gefen *et al* 1983a, Mandelbrot 1982). For the carpet $Q = \ln(b - l)/\ln b$, so it is uniquely defined in terms of b and l.

Lacunarity (L) indicates the degree of translational variance of the fractal set (Mandelbrot 1982). Two carpets with the same b and l (i.e. the same D and Q) can have different distributions of the eliminated squares which result in different degrees of non-translational invariance. Mandelbrot and co-workers (Gefen *et al* 1984) gave an approximate expression to evaluate L for the carpet. They consider all possible choices of an $l \times l$ square on the $b \times b$ lattice. For a given choice i, we denote by n_i the number of uneliminated 1×1 squares belonging to the $l \times l$ square. Then the lacunarity is defined by

$$L^{(1)} = \frac{1}{N} \sum_i (n_i - \bar{n})^2 \qquad \bar{n} = \frac{\Sigma_i n_i}{N} \tag{2.2}$$

with N being the total number of choices of the $l \times l$ square out of $b \times b$. The above formula is only approximate and it actually gives $L = 0$ for some carpets which are obviously not translationally invariant (see figure 1). The reason for the inaccuracy of the definition is that it uses only one stage in the construction of the carpet. A

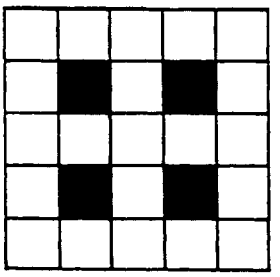

Figure 1. Sierpinski carpet (5, 2) with scattered cutout. $n_i = 3$ for all i. Thus $L = 0$ according to equations (2.2) and (2.3).

better definition would take many stages into consideration. It was claimed (Gefen *et al* 1983c) that on a Sierpinski carpet, critical properties approach that of the hypercubic lattice of the same dimension when $L \to 0$. In that paper (Gefen *et al* 1983c), lacunarity is defined as the mean square deviation divided by the square of the mean. One can define

$$L^{(2)} = \frac{1}{N} \sum_i \left(\frac{n_i}{\bar{n}} - 1 \right)^2 . \tag{2.3}$$

In the following we will refer to these two definitions of lacunarity.

The second definition seems more appropriate for the following reason: if one considers Sierpinski carpets with scattered cutout (as depicted in figure 1) with $b = 2l + 1$, one expects that, as $b \to \infty$, the carpet looks more and more uniform and $L \to 0$. But numerical results give $L^{(1)} \to \infty$ whereas $L^{(2)} \to 0$ as b becomes large which suggests that $L^{(1)}$ is not properly normalised.

3. Potts lattice gas model

We consider the Potts lattice gas (PLG) Hamiltonian (Nienhuis *et al* 1979)

$$-\frac{H}{kT} = J \sum_{\langle ij \rangle} t_i t_j (\delta_{\sigma_i \sigma_j} - 1) - \tfrac{1}{2} F \sum_{\langle ij \rangle} (t_i - t_j)^2 + G \sum_i t_i \tag{3.1}$$

where σ_i is the Potts spin variable which can take q values and t_i is the lattice gas variable: $t_i = 1$ when site i is occupied by a spin (σ_i) and $t_i = 0$ for a vacant site. J is the spin-spin coupling, F is the lattice gas coupling and G controls the concentration of vacancies. When $G \to \infty$ the model reduces to the undilute Potts model.

As noted in the introduction, when using a real space renormalisation procedure it is imperative to use the dilute Potts model in order to detect a first-order transition, even on ordinary lattices (Nienhuis *et al* 1979, Andelman and Berker 1981) since without dilution the renormalisation group does not respect the symmetry of the various degenerate ground states which coexist at the transition.

The same phenomenon occurs for fractal lattices, hence the necessity to consider the Potts lattice gas instead of the pure Potts model in order to determine q_c—the value of q below which the transition is second order and above which the transition is first order. Also in this case the exponents obtained for $q \leqslant q_c$ are more accurate than those obtained using the pure model. Another obvious advantage is, of course,

the calculation for $q \leqslant q_c$ of the tricritical exponents, since tricritical behaviour exists only for the dilute model.

We studied the critical properties of the PLG on Sierpinski carpets using the Migdal-Kadanoff (Migdal 1975, Kadanoff 1976) bond-moving approximation which is essentially a one-dimensional decimation method.

We first give here the formula for a one-dimensional decimation with a scale factor of N. Defining

$$x \equiv e^{-J} \qquad f = e^{-F} \qquad g = e^{-G} \tag{3.2}$$

the renormalised couplings are given by (Berker *et al* 1980)

$$\begin{aligned}(x')^{-1} &= \frac{qR_0 + q - 1}{qR_0 - 1} \\ (f')^{-1} &= \frac{R_2}{R_1^2}\left(R_0 + 1 - \frac{1}{q}\right) \\ (g')^{-1} &= \frac{1}{R_2}\left(R_0 + 1 - \frac{1}{q}\right)\end{aligned} \tag{3.3}$$

with

$$\begin{aligned}R_n &= \frac{x_+^N A_+^n}{q + A_+^2} + \frac{x_-^N A_-^n}{q + A_-^2} \\ A_\pm &= w \pm (q + w^2)^{1/2} \\ w &= f^{-1/2}[g^{1/2} - g^{-1/2}(1 - x + qx)]/2 \\ x_\pm &= (g - f^{1/2} g^{1/2} A_\mp)/(1 - x).\end{aligned} \tag{3.4}$$

4. Renormalisation scheme

We outline in this section the renormalisation group procedure for the Sierpinski carpet with a central cutout, using the bond moving technique. The procedure for other types of carpets is outlined in appendix 2.

The bond moving scheme is similar to the one used in Gefen *et al* (1984), but here we have additional bond and on-site couplings. The on-site couplings are not moved. All the interior bonds within the $b \times b$ cells are moved to the edges in a symmetrical way (see figure 2). The renormalisation scheme compels us to introduce two types of bonds with couplings

$$x = e^{-J} \qquad f = e^{-F} \qquad \text{and} \qquad x_w = e^{-J_w} \qquad f_w = e^{-F_w}. \tag{4.1}$$

The latter couplings belong to bonds which are part of a wall, i.e. to an edge of a cutout. We will argue in the following that it is also necessary to introduce two kinds of on-site couplings g and g_w. In figure 2 we show the two types of bonds: normal type and wall type after bond moving. In the first stage one decimates the $(b-l)/2$ bonds in the two exterior sections and the l bonds in the intermediate section. The three sections are then combined into a single renormalised bond with parameters x',

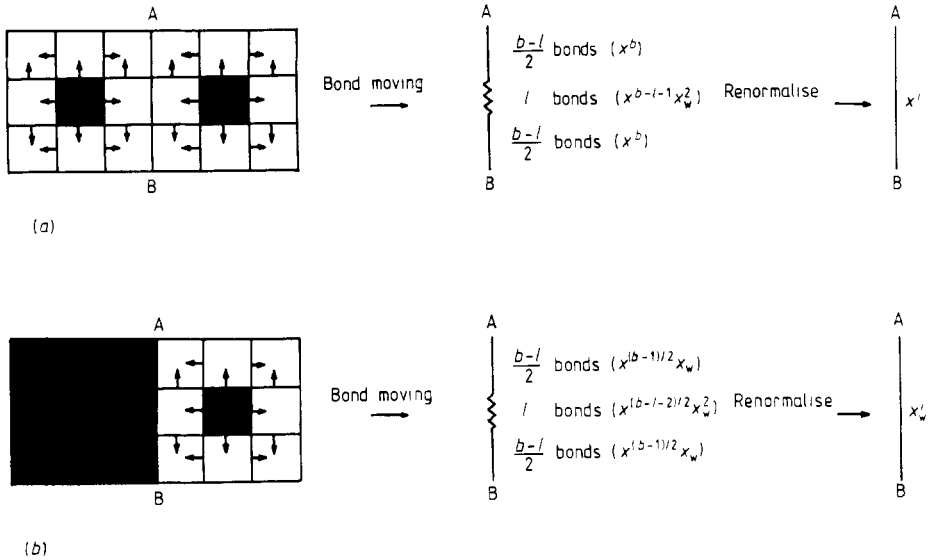

Figure 2. Bond moving renormalisation scheme for a Sierpinski carpet with central cutout. The direction of bond moving is always outwards and bonds are moved to overlap on bonds of the next stage. (*a*) Normal bond. (*b*) Wall bond. $x = e^{-J}$, $x_w = e^{-J_w}$ and $f = e^{-F}$, $f_w = e^{-F_w}$ are treated in the same way, but $g = e^{-G}$, $g_w = {}^{-G_w}$ are not moved. The strength of each bond is given in parentheses.

f', $\bar{g}$ or x'_w, f'_w, $\bar{g}_w$ for normal type or wall type respectively. The formula for adding the three sections is given in appendix 1. The couplings $\bar{g}$ and $\bar{g}_w$ are not yet the renormalised coupling constants g' and g'_w. The renormalised couplings are given by

$$g' = \bar{g}^2/g \qquad g'_w = \bar{g}_w(\bar{g}/g)^{1/2}. \tag{4.2}$$

To derive (4.2) one realises, looking at the geometry of the carpet, that it is natural to define three types of on-site couplings which may be denoted by ○, △, × (see figure 3(*a*)). The site denoted by ○ is a site not attached to a wall, △ denotes a site attached to a wall which is not at a corner of the wall and × denotes a site at a corner of the wall. In our renormalisation procedure bonds are moved but not sites. Hence, considering two types of bonds after bond moving (figure 3(*b*)) with ○ type or △ type on-site couplings respectively, they yield after decimation to bonds with end-site coupling of type $\bar{\bigcirc}$ and $\bar{\triangle}$, respectively. Thus the renormalisation of the various couplings will be

$$\begin{aligned} \bigcirc' &= 2\bar{\bigcirc} - \bigcirc \\ \triangle' &= \bar{\triangle} + \tfrac{1}{2}\bar{\bigcirc} - \tfrac{1}{2}\bigcirc \\ \times' &= \times + \bar{\bigcirc} - \bigcirc + \bar{\triangle} - \triangle \end{aligned} \tag{4.3}$$

and the first two relations are independent of ×. Thus we consider only the couplings corresponding to $\bigcirc(G)$ or $\triangle(G_w)$ and by using the definition $g = \exp(-G)$, $g_w = \exp(-G_w)$ we arrive at (4.2). Note that at the fixed point $g' = g = g^*$ one has also $\bar{g} = g^*$ and similarly $\bar{g}_w = g_w^*$. Thus we could have used $\bar{g}$ and $\bar{g}_w$ to locate the fixed points. The eigenvalues of the RG iterations about the fixed point depend though on the form of (4.2).

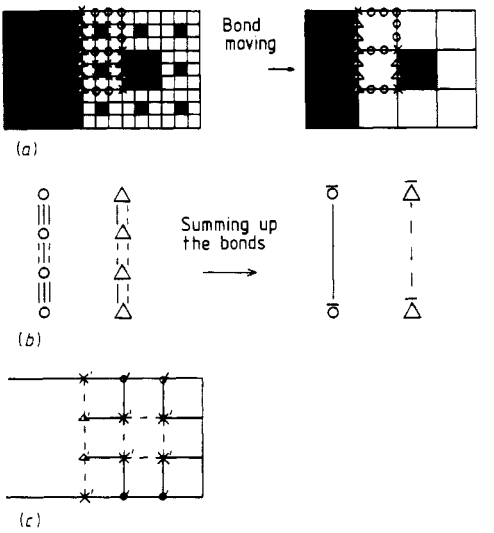

Figure 3. Renormalisation of the on-site coupling. For simplicity, the carpet (3, 1) is drawn as an illustration. (*a*) Labels for the three different types of sites; (*b*) the two types of bonds arising from bond moving. Full and broken lines denote normal wall bonds respectively; (*c*) situation after one complete renormalisation. The cutouts are not shaded for better visualisation of the bonds and sites.

The renormalisation procedure is performed numerically on the computer by using the analytic formulae discussed above. One subroutine performs the decimation of bonds of equal strength to arrive at the three sectors depicted in figure 2. Another subroutine adds the three bonds of which the first and third have the same strength. And thus, with the use of (4.2) the renormalised couplings are being obtained after a single iteration of scale factor b.

It is possible to improve sometimes the results of the Migdal-Kadanoff recursion relations (Andelman and Berker 1981) by shrinking the lattice after each iteration to keep the density of sites fixed. Since sites are not moved together with the bonds the number of sites decreases after each iteration. It is possible to compensate for this decrease in density by shrinking the size of the carpet appropriately. The shrinking factor z for the case of a central cutout is worked out in appendix 3 and is given by

$$z=\left(1-\frac{b+l-2}{(b+l)[1+2l/(b^2-l^2-b)-1/(b^2-l^2-1)]}\right)^{1/D}. \tag{4.4}$$

To summarise, we obtained six recursion relations of the form

$$x'=x'(x, x_w, f, f_w, g, g_w)$$

etc. It is possible to construct a map of the flow in the six-dimensional space, but this method is very awkward because of the high dimensionality and the fact that most fixed points have unstable directions. It is much better to use a Newton-Raphson type routine for finding zeros of a set of non-linear equations of the form

$$x'-x'(x, x_w, f, f_w, g, g_w)=0$$

etc, and then find the eigenvalues of the recursion relations about these fixed points. This is the procedure we followed.

5. Results

As outlined in § 4, the six non-linear equations are solved numerically, and the fixed points are found for a given carpet, for various values of q—the number of Potts states. In most of the following we discuss the case of the central cutout with $b > l+2$, and the case of scattered cutout such that holes are separated by at least two non-eliminated squares. Other cases are discussed in appendix 4. A typical plot of the x^* fixed point value against q is depicted in figure 4. For small values of q we find both a critical and a tricritical fixed point. They merge for some value of q denoted by q_c. For the critical fixed point $g_w^* \sim 0$ which means that there are no vacancies on the walls. We also show the undiluted fixed point $g^* = g_w^* = 0$ which is obtained for the undiluted model. As discussed previously, in the undiluted case one cannot observe the first-order transition for any value of q, since the recursion relations do not preserve correctly the symmetry of the coexisting phases at the transition. Also shown in the figure is a broken curve which connects the point where the critical and tricritical points merge to the line of undiluted fixed points. This line is most probably spurious and is an artefact of the renormalisation procedure and does not represent any real physics. We do not consider it further in the following discussion.

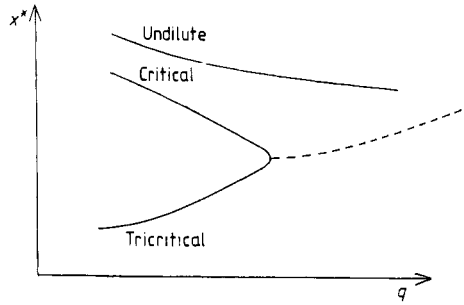

Figure 4. Typical fixed point locus of Sierpinski carpet considered in § 5.

We obtained the critical and tricritical fixed points for several values of (b, l) and for different values of q as displayed in figure 5. We observed that $g^t > g^c$ and $g_w^t > g_w^c \sim 0$, i.e. the tricritical point is characterised by a higher concentration of vacancies, as is also true for an ordinary cubic lattice.

Table 1 shows the critical exponent as obtained from the undilute model using Migdal RG as opposed to the two leading critical exponents obtained from the Potts lattice gas for the cases $q = 2$ and $q = 5$. For $q = 2$ the results obtained from the two models agree closely, but for $q = 5$ which is closer to q_c the deviations are larger. The undiluted case will continue to show a second-order transition even for $q > q_c$. Notice that it is the second leading exponent for the PLG which corresponds to the thermal exponent since its eigenvector lies mostly in the x or x_w direction, whereas the leading exponent corresponds to an eigenvector which points in another direction in parameter space.

In figure 6, q_c is plotted against the fractal dimension D for various values of b and l. We notice that, contrary to the hypercubic lattice, q_c is not a monotonically decreasing function of D. One reason is due to the inaccuracies associated with the Migdal scheme. Returning to the hypercubic lattice we verified that q_c is sensitve to

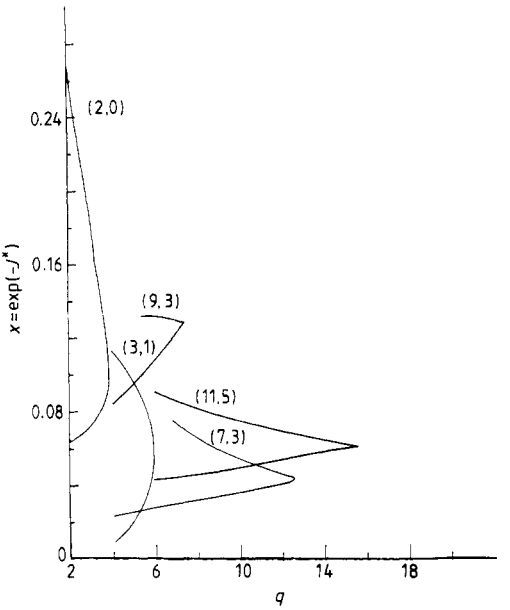

Figure 5. Value of the fixed point x^* plotted against q for various (b, l).

Table 1. Comparison between the critical exponents of undilute (UDL) and PLG models. y_{UDL} should be compared with the second leading y^c_{PLG} since the leading one has an eigendirection which has vanishing x or x_w components.

	$q=2$			$q=5$		
(b, l)	y_{UDL}	y^c_{PLG} (first two leading)		y_{UDL}	y^c_{PLG} (first two leading)	
(5, 1)	0.519	1.296	0.487	0.619	1.134	0.271
(7, 3)	0.314	1.308	0.278	0.330	1.233	0.284
(9, 3)	0.432	1.253	0.419	0.504	1.171	0.347
(11, 5)	0.342	1.256	0.340	0.392	1.217	0.311
(16, 8)	0.341	1.228	0.321	0.400	1.203	0.309
(15, 7)	0.357	1.228	0.342	0.419	1.198	0.325

the scale factor b for a fixed dimension of the hypercubic lattice. In the case of the hypercubic lattice one can always choose a small value of the scale factor $b > 1$ in the Migdal scheme. But for the fractal lattice we must take the scale factor to be equal (at least) to the value of b which defines the carpet, otherwise self-similarity will be lost. One observes that q_c for the carpet is larger than q_c for the hypercubic lattice of the same dimension when one uses the same scale factor b.

It was suggested by Gefen *et al* (1984) that lacunarity is an additional parameter which distinguishes fractal lattices with the same value of D, and certain properties of spin models on fractals may depend on the lacunarity L even for the same value of D and Q (which are both uniquely determined by b and l). Hence universality may be lost and critical properties of the fractal may coincide with the characteristics of a hypercubic lattice of the same dimension only in the limit of low lacunarity (Gefen

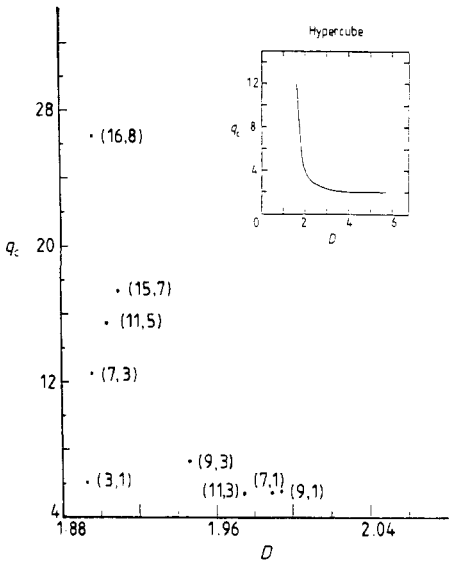

Figure 6. q_c plotted against D for Sierpinski carpets and for the hypercube.

et al 1983c). In order to isolate the dependence of q_c on L one has to fix b and l and look at carpets with a different distribution of cutouts. The four carpets (8, 2) shown in figure 7 have the same D and Q but different lacunarity. Figure 8 shows a plot of q_c against $L^{(2)}$ (using the definition (2.3) of lacunarity). q_c increases only slightly with L and is almost constant. This suggests that q_c is rather insensitve to lacunarity.

To investigate the effect of lacunarity on the critical exponents of the carpet, we have chosen various values of b and l all corresponding to $D \sim 1.9$, and all having roughly the same value of Q. The results are given in table 2 with lacunarity calculated using the two definitions given in § 2. According to definition (1), these carpets have a wide range of lacunarity and the exponents stay almost constant over this range of three decades. However, if one looks at values of lacunarity using definition (2), all these carpets have very close values of the lacunarity $L^{(2)} \sim 0.12$.

To isolate the effect of lacunarity, we again consider the carpets depicted in figure 7. The corresponding exponents are calculated, and the results are tabulated in table 3. A plot of the thermal exponent (which is the second leading exponent) against $L^{(2)}$ is shown in figure 9. The critical exponents show a very slight rise as the lacunarity increases. It is not clear if this rise is intrinsically related to lacunarity or is associated with the approximations involved in the Migdal scheme. In any case lacunarity does not emerge as a strong factor in determining the critical properties. Similar conclusions will be reached in the next section where we carry out a more detailed investigation of the (undiluted) Ising model on a Sierpinski carpet.

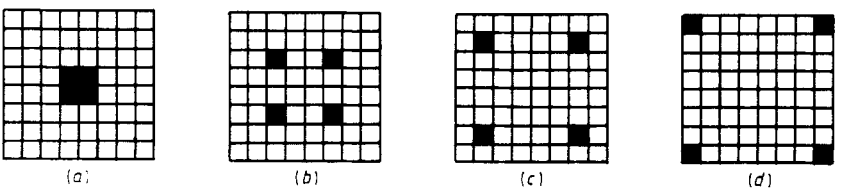

Figure 7. Sierpinski carpets (8, 2) with different lacunarities.

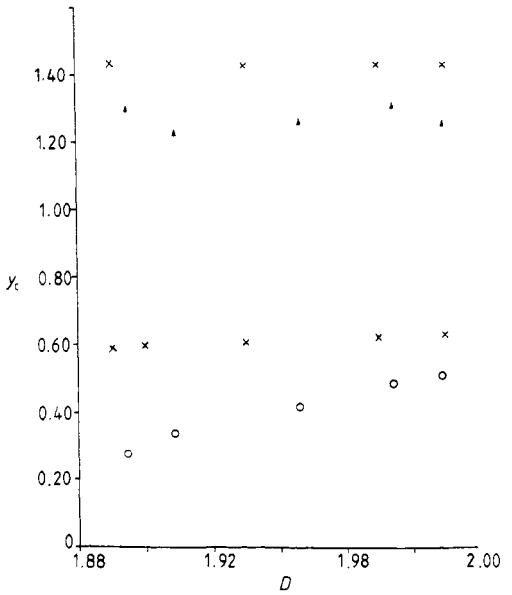

Figure 8. q_c plotted against $L^{(2)}$ for Sierpinski carpets (8, 2). D and Q are constant.

Table 2. Data of PLG on Sierpinski carpets with central cutout. $D \sim 1.9$. c and t denote critical and tricritical points, respectively. y are calculated for $q = 5$, the first three leading y being given here.

(b, l)	D	Q	q_c	$L^{(1)}$	$L^{(2)}$		$y = \ln \lambda / \ln b$ for $q = 5$		
(3, 1)	1.8928	0.6309	6.1	0.098 77	0.1250	c	1.195	0.308	−0.190
						t	1.437	0.616	0.148
(7, 3)	1.8957	0.7124	12.5	3.942 4	0.1188	c	1.233	0.284	−0.099
						t	1.303	0.661	0.291
(11, 5)	1.9035	0.7472	15.5	24.040	0.1192	c	1.217	0.311	−0.120
						t	1.249	0.649	0.317
(15, 7)	1.9093	0.7679	17.4	81.896	0.1196	c	1.198	0.325	−0.145
						t	1.220	0.646	0.326
(16, 8)	1.8962	0.7500	26.5	118.38	0.1263	c	1.203	0.309	−0.170
						t	1.223	0.707	0.320
(20, 10)	1.8910	0.7686	27.0	277.58	0.1251	c	1.188	0.318	−0.168
						t	1.198	0.693	0.326
(21, 11)	1.8947	0.7563	37.5	357.24	0.1293	c	1.190	0.310	−0.165
						t	1.202	0.729	0.321
(25, 13)	1.9021	0.7720	38.5	692.61	0.1280	c	1.177	0.319	−0.189
						t	1.187	0.715	0.326
(26, 14)	1.8949	0.7627	52.0	838.93	0.1310	c	1.178	0.314	-0.194
						t	1.188	0.735	0.322
(31, 17)	1.8958	0.7685	64.0	1687.0	0.1321	c	1.169	0.319	−0.178
						t	1.178	0.741	0.324

Table 3. Data of PLG on Sierpinski carpets in figure 7.

Figure	q_c	$L^{(1)}$	$L^{(2)}$		y for $q=5$ (first three leading)		
(*a*)	6.0	0.6281	0.046 54	c	1.137	0.330	−0.218
				t	1.173	0.403	0.191
(*b*)	5.9	0.2200	0.016 3		1.101	0.301	−0.267
					1.167	0.420	0.152
(*c*)	5.9	0.2200	0.016 3		1.084	0.293	−0.245
					1.141	0.419	0.146
(*d*)	5.5	0.0747	0.004 87		1.071	0.268	−0.197
					1.079	0.331	0.115

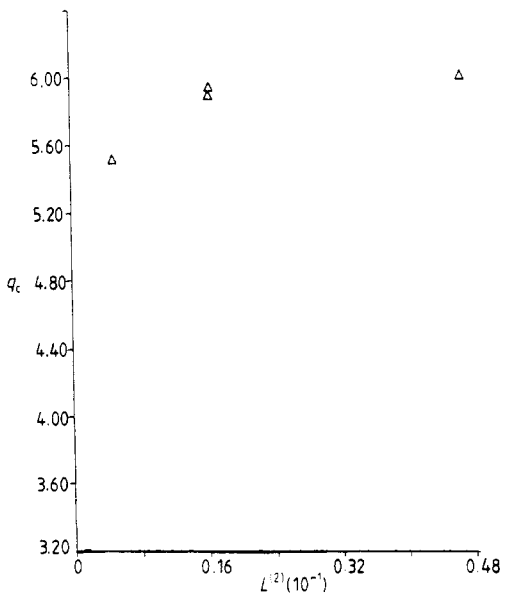

Figure 9. Critical (●) and tricritical (△) exponents plotted against $L^{(2)}$ for Sierpinski carpet (8, 2). For the critical exponents, the second leading ones are used.

Figure 10 shows the critical and tricritical exponents plotted against D for the case of a central cutout. The hypercubic lattice data are also plotted on the same figure. One should bear in mind that, for the same fractal dimension D, the two lattices differ also in the value of the connectivity which is given by

$$Q = D - 1 \qquad \text{hypercubic lattice}$$

$$Q = D - 1 - \ln(1 + l/b)/\ln b \qquad \text{Sierpinski carpet.}$$

6. The undiluted Ising model on a Sierpinski carpet

This model has been considered in Gefen *et al* (1984), but we try to investigate in greater detail the effect of lacunarity on the critical behaviour and also compare with the results of the diluted model.

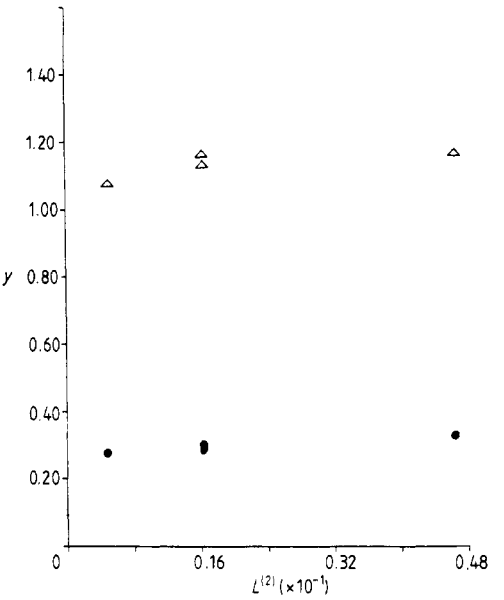

Figure 10. Critical (○) and tricritical (▲) exponents for various Sierpinski carpets plotted against D. For the critical exponents, the second leading ones are used. The critical and tricritical exponents for the hypercube are also shown (×).

In order to investigate the dependence of the critical behaviour on lacunarity, we have tried to keep the fractal dimension D as constant as possible, with $D \sim 1.9$ and $\Delta D/D < 0.5\%$. The connectivity Q is quite constant with $Q \sim 0.75$. We have considered two types of carpets: the carpets with central cutout and those with the scattered cutout (with $b = 2l+1$; l odd). Ising spins have been put on the lattice sites. Migdal's bond moving renormalisation scheme has been used along the lines described in Gefen *et al* (1984). Fixed points and thermal exponents are listed in table 4. Typical renormalisation group flow diagrams are depicted in figure 11. There are always two non-trivial fixed points E and F. $E = (x^*, x_w^* = 0)$ is the same for both central and scattered cutout types with equal values of b and l. E is unstable in both x and x_w directions. For the central cutout type $F = (x^* \neq 0, x_w^* \neq 0)$, and for the scattered cutout type $F = (x^* = 0, x_w^* \neq 0)$. The exponents at E are equal for both types of carpets with the same b and l, but at F the exponent ν is smaller for the central cutout type. For the types of carpets studied in Gefen *et al* (1984) our results agree with those reported there. In order to study the effects of lacunarity on critical exponents, we plot in figure 12 the exponent ν_F against lacunarity, as calculated from the definitions (2.2) and (2.3). Figure 12(a) shows that ν decreases with increasing $L^{(1)}$ for low values of the lacunarity, but stays rather constant over four decades for larger values of L. Figure 12(b) shows the exponent plotted against $L^{(2)}$ as calculated from (2.3). Except for the point corresponding to the carpet characterised by $(b, l) = (3, 1)$ (for which the connectivity Q is exceptionally low) ν stays quite constant with a value $\nu \sim 1.9$. Both definitions suggest that ν is rather insensitve to lacunarity.

Also from table 4, one can see that, for data with almost identical D and $L^{(2)}$, ν decreases as Q increases. To summarise one can deduce the following variation of ν from table 4 (in each case the other unmentioned quantities are held constant):

(i) ν increases with decreasing D,

Table 4. Undilute Ising model on Sierpinski carpets. Density of sites is not conserved. The thermal exponent ν is given by y_1^{-1}.

(b, l)	D	Q		$x^* = e^{-J^*}$	x_w^*	$L^{(1)}$	$L^{(2)}$	y_1^{-1}	y_2^{-1}
Central cutout									
(3, 1)	1.893	0.631	F	0.177	0.969	0.098 77	0.125	4.46	−7.30
			E	0.786	0			1.78	2.43
(7, 3)	1.876	0.712		0.577	0.991	3.942	0.119	1.91	−0.69
				0.841	0			1.68	2.25
(11, 5)	1.904	0.747		0.683	0.998	24.04	0.119	1.82	−0.57
				0.871	0			1.67	2.18
(15, 7)	1.909	0.768		0.741	0.9993	81.90	0.120	1.79	−0.51
				0.891	0			1.67	2.13
(16, 8)	1.896	0.750		0.729	0.9993	118.4	0.126	1.84	−0.53
				0.899	0			1.70	2.17
(20, 10)	1.904	0.769		0.771	0.9998	277.6	0.125	1.82	−0.48
				0.910	0			1.70	2.13
(21, 11)	1.895	0.756		0.763	0.9998	387.2	0.129	1.85	−0.49
				0.915	0			1.71	2.15
(24, 12)	1.909	0.782		0.801	0.9999	560.8	0.124	1.81	−0.43
				0.919	0			1.70	2.10
(25, 13)	1.902	0.772		0.795	0.9999	692.6	0.128	1.83	−0.46
				0.922	0			1.71	2.12
(26, 14)	1.895	0.763		0.790	0.9999	838.9	0.131	1.85	−0.41
				0.926	0			1.73	2.14
(29, 15)	1.908	0.784		0.818	0.999 97	1222.9	0.127	1.83	−0.42
				0.929	0			1.72	2.10
(30, 16)	1.902	0.776		0.814	0.999 97	1445.5	0.130	1.84	−0.41
				0.931	0			1.73	2.11
(31, 17)	1.876	0.769		0.810	0.999 97	1687.0	0.132	1.85	−0.44
				0.934	0			1.74	2.13
(32, 18)	1.890	0.761		0.807	0.999 97	1947.4	0.134	1.86	−0.42
				0.936	0			1.75	2.14
Scattered cutout									
(7, 3)	1.876	0.712		0	0.747	0.9984	0.020 15	2.17	−2.99
				0.841	0			1.68	2.25
(11, 5)	1.904	0.747		0	0.764	2.949	0.008 08	1.97	−2.21
				0.871	0			1.67	2.18
(15, 7)	1.909	0.768		0	0.790	5.920	0.004 29	1.91	−2.00
				0.891	0			1.67	2.13

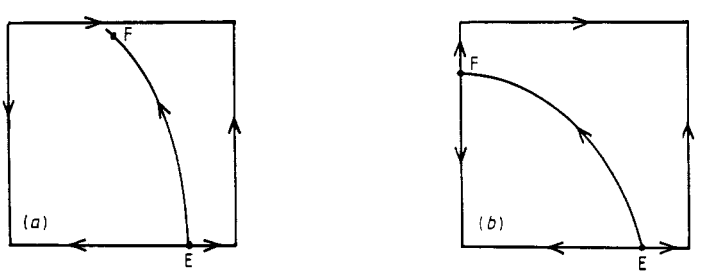

Figure 11. Flow diagram of Sierpinski carpet (7, 3). (*a*) Central cutout; (*b*) scattered cutout.

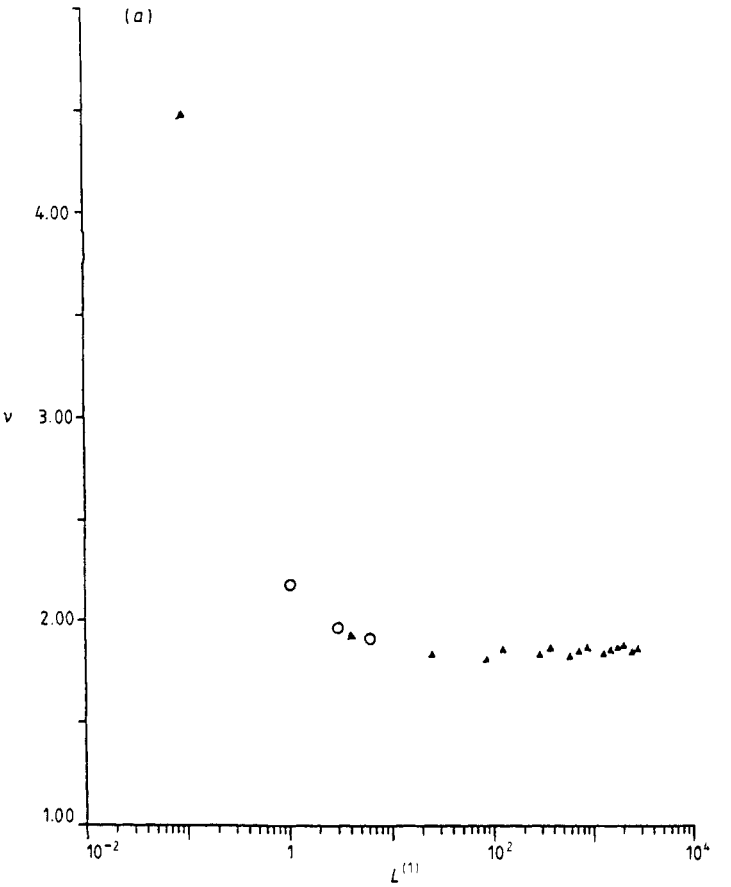

Figure 12. ν plotted against lacunarity for $q = 2$ and $D \sim 1.9$. (*a*) $L^{(1)}$ using equation (2.2); (*b*) $L^{(2)}$ using equation (2.3). ▲, Central; ○, scattered.

(ii) ν increases with decreasing Q,

(iii) ν increases with decreasing L but is rather insensitive to L: $|\partial\nu/\partial L|/|\partial\nu/\partial D| \ll 1$.

Since the bond moving scheme has some intrinsic approximations it is hard to tell whether some of the qualitative results are not affected by them. For example we tried to see how these results will change by modifying the renormalisation group procedure such that the density of sites will be conserved. This is important when one considers the dilute model (Andelman and Berker 1981) and it gives a more accurate value of q_c for the Potts model on the hypercubic lattice. It is thus of interest to see the effect of imposing such a condition in the undilute case. The results can also be more readily compared with those obtained for the diluted model with $q = 2$.

The results for the Ising spin on the carpet with the density of sites conserved are listed in table 5 and flow diagrams are depicted in figure 13. The flow diagrams for the central cutout case are qualitatively the same as for the non-conserved case. For the carpet with scattered cutout though, the fixed point F is characterised by $x^* \neq 0$ as opposed to the non-conserved case where it had $x^* = 0$.

Figure 14 shows a plot of ν_F against $L^{(2)}$ and one observes that ν_F is rather insensitive to lacunarity. For the same values of b and l (hence identical Q and D)

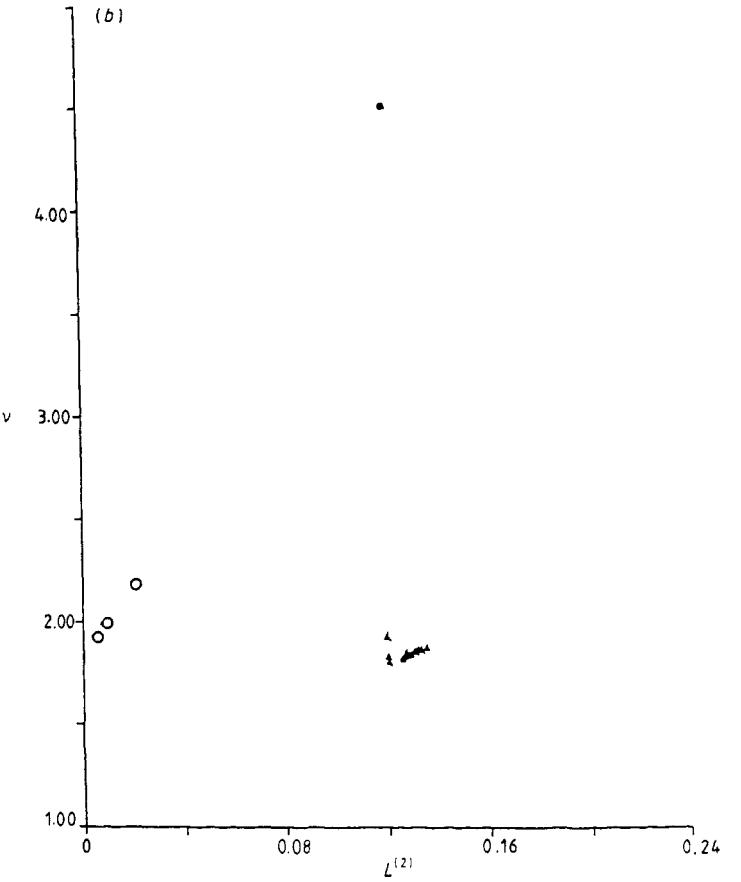

Figure 12. (continued)

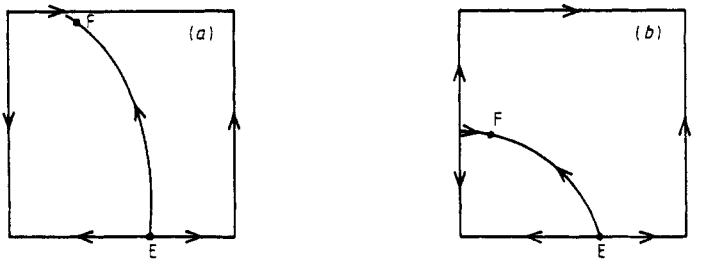

Figure 13. Flow diagram of Sierpinski carpet (7, 3) with density of sites conserved. (*a*) Central cutout; (*b*) scattered cutout.

one finds $\nu_{\text{central}} > \nu_{\text{scattered}}$ in contrast to the results obtained by not conserving the density of sites.

To summarise, both tables 4 and 5 suggest that lacunarity has little effect on the exponents, and it is not clear if the dependence is intrinsic or results from approximations inherent in the Migdal scheme.

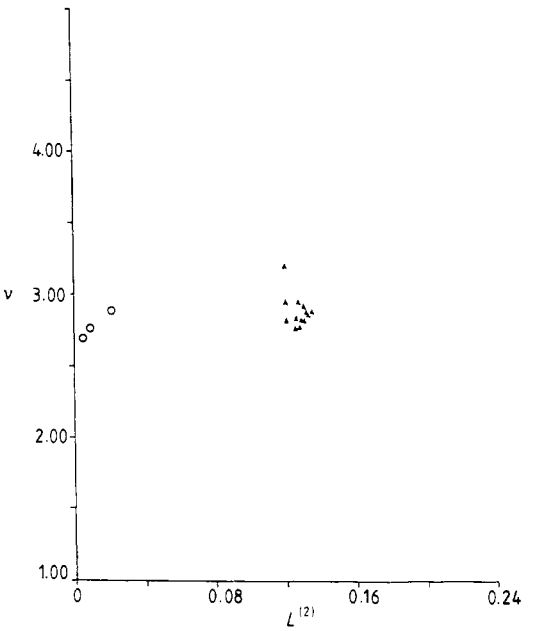

Figure 14. ν plotted against $L^{(2)}$ for $q = 2$ and $D \sim 1.9$, with density of sites conserved.

7. Conclusions

In this paper we have investigated the properties of the Potts model on a fractal lattice with an infinite order of ramification, namely the Sierpinski carpet. The value of q_c, critical and tricritical exponents were obtained for different values of b and l characterising the carpet, and for different distributions of cutouts. The results certainly depend on the fractal dimension D of the fractal. q_c tends to increase very slightly and the exponent ν tends to decrease slightly with increasing lacunarity. But since the Migdal scheme is approximate it would be important to verify these results using a different RG scheme in order to ensure that these small effects are not related to inaccuracies of the RG method. The connectivity is another property which may affect critical behaviour, but a detailed study of its influence is difficult since it is hard to change the connectivity keeping the fractal dimension and lacunarity fixed.

Acknowledgment

This work has been supported by the National Science Foundation under grant no DMR-8302323.

Appendix 1

After bond moving, one obtains the situation represented diagrammatically as in figure 2. Summing up the bonds to get the renormalised couplings is equivalent to multiplying all the transfer matrices (a total of b matrices). Due to the non-commutativity of these transfer matrices of the PLG Hamiltonian, the order of summing the bonds of different

Table 5. Undilute Ising model on Sierpinski carpets. Density of sites is conserved. The thermal exponent ν is given by y_1^{-1}.

(b, l)	D	Q	$x^* = e^{-J^*}$	x_w^*	$L^{(1)}$	$L^{(2)}$	y_1^{-1}	y_2^{-1}
Central cutout								
(3, 1)	1.893	0.631	0.0774	0.643	0.098 77	0.125	2.95	−1.70
			0.695	0			0.44	1.96
(7, 3)	1.896	0.712	0.194	0.888	3.942	0.119	3.18	−1.13
			0.641	0			0.39	1.97
(11, 5)	1.904	0.747	0.268	0.954	24.04	0.119	2.93	−0.91
			0.656	0			0.40	1.99
(15, 7)	1.909	0.768	0.316	0.978	81.90	0.120	2.80	−0.80
			0.670	0			0.40	2.01
(16, 8)	1.896	0.750	0.284	0.974	118.4	0.126	2.93	−0.87
			0.687	0			0.41	2.03
(20, 10)	1.904	0.769	0.327	0.987	277.6	0.125	2.82	−0.77
			0.694	0			0.41	2.04
(21, 11)	1.895	0.756	0.305	0.986	357.2	0.129	2.90	−0.80
			0.706	0			0.41	2.06
(24, 12)	1.909	0.792	0.360	0.993	560.5	0.124	2.75	−0.71
			0.702	0			0.41	2.06
(25, 13)	1.902	0.772	0.342	0.992	692.6	0.128	2.81	−0.73
			0.711	0			0.42	2.07
(26, 14)	1.895	0.763	0.326	0.972	838.9	0.131	2.86	−0.75
			0.719	0			0.42	2.08
(29, 15)	1.908	0.784	0.371	0.996	1222.9	0.127	2.76	−0.69
			0.716	0			0.42	2.08
(30, 16)	1.902	0.776	0.357	0.996	1445.5	0.130	2.79	−0.68
			0.723	0			0.42	2.09
(31, 17)	1.896	0.769	0.344	0.996	1687.0	0.132	2.84	−0.69
			0.730	0			0.42	2.10
(32, 18)	1.890	0.761	0.332	0.996	1947.4	0.134	2.87	−0.71
			0.737	0			0.42	2.11
Scattered cutout								
(7, 3)	1.896	0.712	0.018	0.408	0.9984	0.020 15	2.87	−2.94
			0.647	0			0.40	1.96
(11, 5)	1.904	0.747	0.0103	0.393	2.949	0.008 08	2.74	−2.94
			0.661	0			0.40	1.98
(15, 7)	1.909	0.768	0.008 29	0.403	5.920	0.004 29	2.68	−2.83
			0.673	0			0.41	2.00

strengths cannot be altered. To sum the bonds, the first and last $\frac{1}{2}(b-l)$ bonds are summed by one-dimensional decimation to give a bond of strength x_1; the middle l bonds are similarly decimated to give x_2. We then have the situation of three bonds x_1, x_2, x_1 in series where $x_1 \neq x_2$ in general. The final renormalised coupling x' is obtained by multiplying three transfer matrices of which the middle matrix has different couplings.

The formulae for renormalised couplings x', f', g' ($x = e^{-J}$, $f = e^{-F}$, $g = e^{-G}$) are as follows:

$$x' = \{2x_1 + x_2 + (q-2)x_1^2 + 2(q-2)x_1x_2 + (q^2-3q+3)x_1^2x_2 + 2(f_1f_2g_1g_2)^{1/2}[1+(q-1)x_1] + f_1g_1g_2\}A^{-1}$$

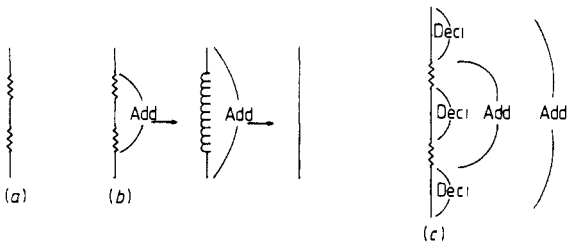

Figure A1. (*a*) Situation after bond moving for the carpet in figure 1. (*b*) Renormalisation procedure for figure 1. (*c*) Renormalisation procedure for figure 7(*b*).

$$f' = \frac{\{g_1g_2\sqrt{f_1} + qf_1(f_2g_1g_2)^{1/2} + [1+(q-1)x_1][(1+(q-1)x_2)\sqrt{f_1} + (g_1g_2f_2)^{1/2}]\}^2}{[\![g_1g_2 + q\{2(f_1f_2g_1g_2)^{1/2} + f_1[1+(q-1)x_2]\}]\!]A} \tag{A1.1}$$

$$g' = g_1[\![g_1g_2 + q\{2(f_1f_2g_1g_2)^{1/2} + f_1[1+(q-1)x_2]\}]\!]A^{-1}$$

where we defined

$$A \equiv 1 + 2(q-1)x_1x_2 + (q-1)x_1^2[1+(q-2)x_2] + 2(f_1f_2g_1g_2)^{1/2}[1+(q-1)x_1] + f_1g_1g_2. \tag{A1.2}$$

Appendix 2

Here we consider Sierpinski carpets such that no two (or more) eliminated units (1×1 squares) are connected with each other and the carpet also respects 90° rotational symmetry. The carpet shown in figure 1 is one example and will be used here as an illustration. After bond moving, one has the situation as in figure A1(*a*). We recall in appendix 1 that one knows how to decimate an arbitrary number of bonds of same strength and one also knows how to add up three bonds such that the first and third bonds have the same strength. We denote the above two tools, respectively, by Deci and Add. The renormalisation procedure is shown diagrammatically in figure A1(*b*). In fact Deci and Add can be used to renormalise any Sierpinski carpet; an example is shown in figure A1(*c*).

Appendix 3

Consider an N-stage Sierpinski carpet with central cutout characterised by b and l. Before bond moving, the total number of sites is

$$(b^N+1)^2 - (lb^{N-1}-1)^2 - (b^2-l^2)(lb^{N-2}-1)^2 - \ldots - (b^2-l^2)^{N-1}(l-1) \xrightarrow{N\to\infty} (b^2-l^2)^N\left(1 + \frac{2l}{b^2-l^2-b} - \frac{1}{b^2-l^2-1}\right). \tag{A3.1}$$

The number of sites decoupled from the lattice upon bond moving is

$$(b^2-l^2)^{N-1}[(b-1)^2-(l-1)^2]. \tag{A3.2}$$

Hence

$$\frac{\text{number of sites after bond moving}}{\text{number of sites before bond moving}}$$

$$= 1 - \frac{(b+l-2)}{(b+l)[1+2l/(b^2-l^2-b)-1/(b^2-l^2-1)]}. \tag{A3.3}$$

If one demands the density of sites to be invariant under bond moving, then one has to shrink the length $b \to \tilde{b}$ such that

$$\frac{\tilde{b}}{b} = \left(1 - \frac{b+l-2}{(b+l)[1+2l/(b^2-l^2-b)-1/(b^2-l^2-1)]}\right)^{1/D} \equiv z \tag{A3.4}$$

i.e. all lengths should be shrunk by a factor of z.

Appendix 4

The type of carpets like the central cutout types with $b = l+2$ (except $b = 3$) and scattered cutout types of the sort in figure 1 are special in terms of the bond moving scheme we used. Consider the situation in figure A2. The middle portion is independent of x, so AB cannot connect even though the normal bond has an infinite strength ($J = \infty$; $x = 0$) and, in this case, critical behaviour is governed by x_w and g_w and there exists fixed values g_w^* other than 0 or 1. Hence, even though q is very large and so one needs a very strong bond for cooperative effect ($x^* \sim 0$), one can still have more than one x_w^*. So the critical and tricritical fixed points do not seem to merge together even for very large q. We believe this is an artefact of the bond moving because actually AB can be connected by normal bonds via paths in higher stages of the carpet.

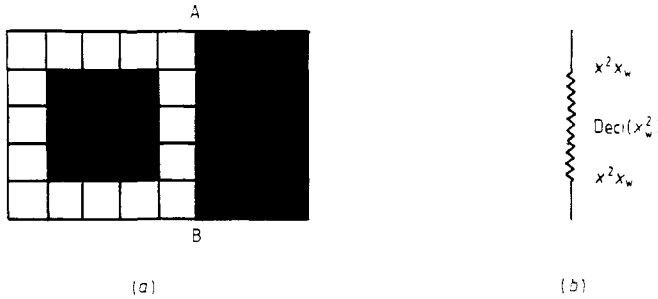

Figure A2. (*a*) Sierpinski carpet (5, 3) with central cutout. (*b*) Situation after bond moving. The strengths of the bonds are shown, the middle portion has been decimated by a scale factor of 3.

References

Andelman D and Berker A N 1981 *J. Phys. A: Math. Gen.* **14** L91
Berker A N, Andelman D and Aharony A 1980 *J. Phys. A: Math. Gen.* **13** L413
Gefen Y, Aharony A and Mandelbrot B B 1983a *J. Phys. A: Math. Gen.* **16** 1267
—— 1984 *J. Phys. A: Math. Gen.* **17** 1277

Gefen Y, Aharony A, Shapir Y and Mandelbrot B B 1983b *J. Phys. A: Math. Gen.* **17** 435
Gefen Y, Meir Y, Aharony A and Mandelbrot B B 1983c *Phys. Rev. Lett.* **50** 145
Kadanoff L P 1976 *Ann. Phys., NY* **100** 359
Mandelbrot B B 1982 *The Fractal Geometry of Nature* (San Francisco: Freeman)
Midgal A A 1975 *Zh. Eksp. Teor. Fiz.* **69** 1457 (*Sov. Phys.-JETP* **42** 743)
Nienhius B, Berker A N, Riedel E K and Schick M 1979 *Phys. Rev. Lett.* **43** 737
Riera R and Chaves C M 1986 *Z. Phys.* B **62** 387